American Mineralogist, Volume 95, pages 933–938, 2010

The crystal chemistry and crystal structure of kuksite, $Pb_3Zn_3Te^{6+}P_2O_{14}$, and a note on the crystal structure of yafsoanite, $(Ca,Pb)_3Zn(TeO_6)_2$

Stuart J. Mills,[1,*] Anthony R. Kampf,[2] Uwe Kolitsch,[3,4] Robert M. Housley,[5] and Mati Raudsepp[1]

[1]Department of Earth and Ocean Sciences, University of British Columbia, Vancouver, British Columbia V6T 1Z4, Canada
[2]Mineral Sciences Department, Natural History Museum of Los Angeles County, 900 Exposition Boulevard, Los Angeles, California 90007, U.S.A
[3]Mineralogisch-Petrographische Abt., Naturhistorisches Museum, Burgring 7, A-1010 Wien, Austria
[4]Institut für Mineralogie und Kristallographie, Geozentrum, Universität Wien, Althanstrasse 14, A-1090 Wien, Austria
[5]Division of Geological and Planetary Sciences, California Institute of Technology, Pasadena, California 91125, U.S.A.

Abstract

New discoveries of kuksite, $Pb_3Zn_3Te^{6+}P_2O_{14}$, from the Black Pine mine, Montana, and Blue Bell claims, California, have enabled a detailed crystal-chemical study of the mineral to be undertaken. Single-crystal X-ray structure refinements of the structure indicate that it is isostructural with dugganite, $Pb_3Zn_3Te^{6+}As_2O_{14}$, and joëlbruggerite, $Pb_3Zn_3(Sb^{5+},Te^{6+})As_2O_{13}(OH,O)$. Kuksite from the Black Pine mine crystallizes in space group $P321$, with unit-cell dimensions a = 8.392(1), c = 5.204(1) Å, V = 317.39(8) Å^3, and Z = 1 (R_1 = 2.91% for 588 reflections [$F_o > 4\sigma F$] and 3.27% for all 624 reflections), while Blue Bell kuksite has the unit cell a = 8.3942(5), c = 5.1847(4) Å, and V = 316.38(4) Å^3 (R_1 = 3.33% for 443 reflections [$F_o > 4\sigma F$] and 3.73% for all 483 reflections). Chemical analyses indicate that solid-solution series exist between kuksite, dugganite, and joëlbruggerite. Raman spectroscopic and powder X-ray diffraction data are also presented for samples from both occurrences.

The crystal structure of the chemically related species yafsoanite, $(Ca,Pb)_3Te^{6+}_2Zn_3O_{12}$, from the type locality (Delbe orebody, Kuranakh Au Deposit, Aldan Shield, Saha Republic, Russia), has been refined to R_1 = 2.41% for 135 reflections [$F_o > 4\sigma F$] and 3.68% for all 193 reflections. A garnet-type structure has been confirmed and significantly improves upon the results of an earlier structure determination.

Keywords: Kuksite, dugganite, joëlbruggerite, Black Pine, Blue Bell, tellurate, yafsoanite, Delbe orebody, crystal structure

Introduction

Tellurium minerals occur in a wide range of environments worldwide, where primary sulfides and sulfosalts have undergone weathering under acidic conditions. Tellurium mineralogy tends to be complex, owing to the various oxidation states possible (Te^{6+}, Te^{4+}, Te^0, and Te^{2-}), which then tend to combine to create many exotic mineral species. Investigations of tellurium mineralogy at the Black Pine mine, 14.5 km NW of Philipsburg, Granite County, Montana [U.S.A. (46°26′52″N, 113°21′56″W)], and the Blue Bell claims, Baker, San Bernardino County, California [U.S.A. (35°14′38″N, 116°12′25″W)], resulted in the discovery of several rare and new tellurate species. One of these rare tellurates, kuksite, $Pb_3Zn_3Te^{6+}P_2O_{14}$, is the subject of this report.

Kuksite is an extremely rare mineral that previously has only been described from its type locality, the Delbe orebody within the Kuranakh Au Deposit, Aldan Shield, Saha Republic, Russia (Kim et al. 1990). Here it occurs as elongated tabular gray crystals up to 0.1 × 0.3 mm with cinnabar, gold, petzite, coloradoite, yafsoanite, kuranakhite, cheremnykhite, descloizite, dugganite, and saponite.

Occurrence and paragenesis

Black Pine mine

Kuksite and associated material was collected in the spring of 1993 by John Dagenais of Vancouver, British Columbia, Canada. Kuksite occurs with malachite, pseudomalachite, chalcocite, tetrahedrite, segnitite, dugganite, and joëlbruggerite in milky quartz veins. Kuksite crystallized from solutions rich in Pb, Zn, Sb, As, P, and Te derived from the breakdown of the primary ore body within the Mount Shields Formation (Peacor et al. 1985; Mills et al. 2009). The tellurium is present in the ore as a substituent in tetrahedrite, a common association in many other deposits (e.g., Fadda et al. 2005). Thermodynamic modeling suggests that kuksite formed in mildly oxidizing [log aO_2(aq) > –41] and acidic conditions (pH < 3), as required for other unique Black Pine minerals such as joëlbruggerite (Mills et al. 2009) and auriacusite (Mills et al. 2010). Synthetic analogues of kuksite can be prepared at >500 °C by solid-state methods (Mill' 2009a, 2009b); however, natural samples have almost certainly crystallized at ambient (~25 °C) temperatures.

Blue Bell claims

Although the Blue Bell mine has been a well-known collecting locality for micro minerals at least since 1977 (Crowley 1977) and 45 minerals from there were described in detail by Maynard (1984), the first tellurate mineral described from the mine, quetzalcoatlite, was collected by one of the authors (R.M.H.) in March of 1996. Shortly following news of this find, kuksite was found in a single Blue Bell specimen submitted to R.M.H. by Eugene Reynolds. These finds were promptly documented in a regional publication (Housley 1997), although the quetzal-

* E-mail: smills@eos.ubc.ca

coatlite was initially misidentified as tlalocite. Subsequently, a crystal of the quetzalcoatlite was used to solve the structure of that mineral (Burns 2000). What is now known as the Blue Bell claims actually consists of a dozen or more small workings distributed over a rugged hillside.

In 2007, R.M.H. found kuksite in material from the Blue Bell D site (Maynard 1984) that had been donated for study by John Jenkins. In March 2008, R.M.H. finally found kuksite in situ in a small adit at the D site. Ironically, somewhat earlier in November 2007, Brent Thorne had independently found larger kuksite crystals associated with quetzalcoatlite in the D site shaft, where quetzalcoatlite had been initially found. He kindly made some of these crystals available for this study in June 2008.

At the Blue Bell the most ubiquitous associates of kuksite are clinochlore, perite, and hemimorphite. Other secondary minerals found in close association include hematite, quartz, wulfenite, chlorargyrite, dioptase, kettnerite, fluorite, murdochite, and very minor calcite, barite, and gypsum. Many chrysocolla pseudomorphs apparently, at least partly, after aurichalcite are also present, as is much gossan. Interestingly, much more Te mineralization is present at this site as green and yellow, X-ray amorphous, opal-like gels consisting of Zn, Cu, Bi, Te, Fe, and Si oxides than the small amount found in well-crystallized minerals.

This part of the Blue Bell claims is located in a skarn area, and although the area appears to be highly oxidized, some small inclusions of primary minerals are trapped in garnet and magnetite of the skarn. These inclusions include sphalerite, bornite, hessite, and tetradymite. Thus, it appears that the suite of secondary minerals including the kuksite could have formed during oxidation of the primary minerals present, with perhaps only Mo and P needing to be derived from the surrounding skarn.

Physical properties

Black Pine mine

Kuksite commonly occurs in various shades of purple, as barrel-shaped or tabular crystals up to about 0.5 mm across (Fig. 1). Forms observed are {0001}, {11$\bar{2}$0}, {10$\bar{1}$0}, and {11$\bar{2}$1}. The barrel-shaped crystals can be randomly color-zoned, with purple, grayish purple, and colorless most prominent. Less commonly, kuksite may occur as bluish or greenish crystals. Visually, kuksite is indistinguishable from the related species dugganite, $Pb_3Zn_3Te^{6+}As_2O_{14}$, and joëlbruggerite, $Pb_3Zn_3(Sb^{5+},Te^{6+})As_2O_{13}(OH,O)$, although joëlbruggerite tends to be an order of magnitude smaller than both kuksite and dugganite.

Blue Bell claims

Kuksite occurs as pale greenish-blue simple stout hexagonal prisms up to about 0.1 mm in length. Forms observed are {0001} and {10$\bar{1}$0}.

Chemical composition

Quantitative analyses (Table 1) of Blue Bell and Black Pine kuksite were performed in wavelength-dispersion (WDS) mode on a JEOL8200 microprobe using a 10 kV electron beam, a 10 nA beam current, and 1–10 µm spot size at the Division of Geological and Planetary Sciences, California Institute of Technology. Probe standards were: PbS (for Pb), Bi-metal (for Bi), ZnO (for Zn), Cu-metal (for Cu), fayalite (for Fe), Te-metal (for Te), Sb-metal (for Sb), fluorapatite (for P), GaAs (for As), and anorthite (for Si). Like many other tellurium oxysalts and dugganite-group members, kuksite is prone to beam damage (including melting observed under stronger analytical conditions) and anomalously low totals (Table 1), cf. Grundler et al. (2008), Mills et al. (2009), and Kampf et al. (2010).

The average of five analyses (calculated on the basis of 14 O) gave the average composition of $Pb_{2.93}(Zn_{2.74}Cu_{0.06}Fe_{0.01})_{\Sigma 2.81}(Te_{0.58}Sb_{0.33})_{\Sigma 0.91}(P_{1.44}As_{0.74}Si_{0.11})_{\Sigma 2.29}O_{14}$ for Black Pine kuksite, while the average of seven analyses gave the average composition of $(Pb_{2.89}Bi_{0.10})_{\Sigma 2.99}(Zn_{2.84}Cu_{0.20}Fe_{0.02})_{\Sigma 3.05}Te_{1.05}(P_{1.52}Si_{0.44}As_{0.02})_{\Sigma 1.98}O_{14}$ for Blue Bell kuksite. The Black Pine kuksite contains substantial As, indicating a solid solution toward dugganite, but also contains substantial Sb toward what would be the Sb analog of kuskite. We note that semi-quantitative SEM analyses show Sb to be low or absent in many samples, indicating multiple generations of formation and/or differing primary minerals to be responsible for formation. Varying Sb is also present in auriacusite and alunite supergroup minerals from Black Pine. The Blue Bell kuksite, on the other hand, shows substantial Si substitution analogous to that reported by Kim et al. (1988).

Raman spectroscopy

Near-infrared Raman spectroscopic analysis was performed using a Renishaw imaging microscope system 1000 (Depart-

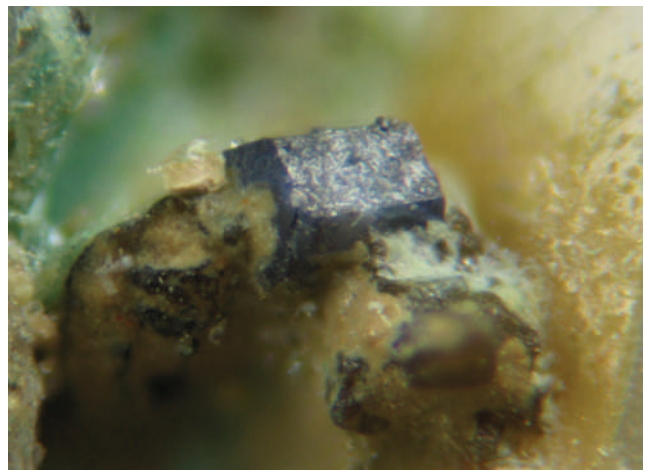

Figure 1. Barrel-shaped crystal of kuksite from the Black Pine mine in quartz vugh. Field of view is 0.3 mm across. Jean-Marc Johannet specimen and photograph.

Table 1. Quantitative chemical analyses for kuksite (average of five analyses for Black Pine and seven for Blue Bell)

wt%	Black Pine	SD	Blue Bell	SD
PbO	50.56	0.64	48.09	1.30
CuO	0.37	0.05	1.16	0.32
FeO	0.06	0.03	0.14	0.13
ZnO	17.26	0.12	17.21	0.54
Bi_2O_3	0.00	0.00	1.78	0.53
V_2O_3	0.01	0.01	0.01	0.02
SiO_2	0.52	0.05	1.99	0.28
P_2O_5	7.93	0.09	8.02	0.42
As_2O_5	6.57	0.35	0.19	0.23
Sb_2O_5	4.14	0.25	0.02	0.04
TeO_3	7.93	0.11	13.74	0.37
Total	95.35		92.35	

ment of Biochemistry, UBC), with a RL785 diode laser at a wavelength of 785 nm, a RenCam CCD detector and Renishaw WiRE Version 1.3.30 instrument control software. The data were analyzed using Galatic Grams/32 Version 4.14 software. Prior to data acquisition, a spectral calibration was carried out using the Raman spectrum obtained from a silicon wafer. Spectra were recorded in backscatter mode between 150 and 3500 cm^{-1} with a spectral resolution of ±2 cm^{-1} and a minimum lateral resolution of ~2 μm on the sample.

The Raman spectrum of kuksite shows the $\nu_3(PO_4)$ vibration at 1006 cm^{-1} for Blue Bell kuskite and 1017 cm^{-1} for Black Pine kuksite. Additional bands, attributed to the $\nu_2(PO_4)$ and $\nu_4(PO_4)$ vibrations, were observed at 497, 476, and 424 cm^{-1} for the Black Pine kuksite and at 529, 493, and 416 cm^{-1} for the Blue Bell kuksite. Bands at 734 cm^{-1} (Blue Bell) and 731 cm^{-1} (Black Pine) are attributed to Te-O lattice vibrations. No band was observed in the hydroxyl region for Black Pine kuksite; however, a small band at 3036 cm^{-1}, attributed to an O-H stretching vibration, was observed for Blue Bell kuksite. The Raman results correlate well with those for joëlbruggerite (Mills et al. 2009).

X-RAY DIFFRACTION

Powder X-ray diffraction

X-ray powder diffraction data (Table 2) were collected on crystal fragments using a Rigaku R-Axis Spider curved imaging plate microdiffractometer utilizing monochromatized Mo$K\alpha$ radiation. The fragments were randomized using a Gandolfi-like motion about two axes (rotation on φ and oscillation on χ). The resulting pattern was integrated using the program AreaMax v2.0 and then analyzed using JADE v9.0. Unit-cell parameters refined from the powder data using Chekcell (Laugier and Bochu 2004) are a = 8.438(7) and c = 5.201(1) Å for Black Pine kuksite and a = 8.394(8) and c = 5.176(2) Å for Blue Bell kuksite, which are in good agreement with those obtained from the single-crystal study (see below).

TABLE 2. Powder X-ray diffraction data for kuksite

	Blue Bell, California*		Black Pine, Missouri†		Kuranakh, Russia‡	
hkl	I_{obs}	d_{obs}	I_{obs}	d_{obs}	I_{obs}	d_{obs}
010	4	7.184				
001	**25**	5.176	16	5.210	20	5.18
011, 110	16	4.191	19	4.226	10	4.25
020	18	3.632	19	3.655	20	3.68
111	**100**	3.258	**100**	3.277	**100**	3.29
021	**83**	2.974	**84**	2.992	**80**	3.00
120	25	2.745	**30**	2.762	20	2.78
002	20	2.589	17	2.602	**40**	2.594
012, 121, 030	25	2.424	30	2.438	20	2.462
112, 031	17	2.199	16	2.210	<10	2.237
022, 220	18	2.107	17	2.118	10	2.121
130	19	2.015	21	2.028	**30**	2.041
221	6	1.944				
122, 131	**47**	1.881	**47**	1.890	**50**	1.903
032	14	1.769	16	1.778	20	1.785
013, 230	6	1.666	5	1.676	10	1.686
112, 132, 231, 140	**44**	1.589	**44**	1.597	30	1.606
023	15	1.558	9	1.567	<10	1.571
123, 050	5	1.456	6	1.463		
033, 232, 051, 330	16	1.400	16	1.407		
240			4	1.379		
223			5	1.336		
133	8	1.310	6	1.318		
014, 052, 151	8	1.267	9	1.273		

Note: Five strongest lines are in boldface; indexing based on powder pattern calculated from the single-crystal structure models.
* Refined unit-cell parameters: a = 8.394(8), c = 5.176(2) Å.
† Refined unit-cell parameters: a = 8.438(7), c = 5.201(1) Å.
‡ Data from Kim et al. (1990); cell parameters: a = 8.50(3), b = 14.72(5), c = 5.19(3) Å.

Single-crystal X-ray diffraction

The single-crystal study of Black Pine kuksite was undertaken using a Nonius KappaCCD single-crystal diffractometer equipped with a 300 μm diameter capillary-optics collimator to provide increased resolution. An optically homogeneous, barrel-shaped crystal with the dimensions 0.08 × 0.08 × 0.02 mm was used for collection of intensity data at 293 K (Table 3). The intensity data were processed with the Nonius program suite DENZO-SMN and corrected for Lorentz, polarization, and background effects, and, by the multi-scan method (Otwinowski and Minor 1997; Otwinowski et al. 2003), for absorption. The single-crystal study of Blue Bell kuksite was undertaken using a Rigaku R-Axis Spider curved imaging plate microdiffractometer utilizing monochromatized Mo$K\alpha$ radiation. The Rigaku Crystal Clear software package was used for processing of the structure data.

The crystal structure of kuksite was solved in $P321$ (no. 150), by direct methods using SHELXS-97 (Sheldrick 2008) and subsequent Fourier and difference Fourier syntheses, followed by anisotropic full-matrix least-squares refinements on F^2 using SHELXL-97 (Sheldrick 2008). The models were then compared to those of joëlbruggerite (Mills et al. 2009) and dugganite (Lam et al. 1998). The final model converged to R_1 = 2.91% for 588 reflections [$F_o > 4\sigma F$] and 3.27% for all 624 reflections for the Black Pine crystal and to R_1 = 3.36% for 445 reflections [$F_o > 4\sigma F$] and 3.80% for all 485 reflections for the Blue Bell sample. Details of the data collections and refinements are given in Table 3. The refined atomic coordinates, site occupancies, and

TABLE 3. Summary of data collection conditions and refinement parameters for kuksite

	Black Pine	Blue Bell
Structural formula	$Pb_3Zn_3Te^{6+}(P_{1.59}As_{0.41})_{\Sigma 2}O_{14}$	$Pb_3Zn_3Te^{6+}(P_{1.33}Si_{0.67})_{\Sigma 2}O_{14}$
Temperature (K)	293(2)	293(2)
Wavelength (Å)	0.710747	0.710747
Space group	$P321$	$P321$
Unit-cell dimensions	a = 8.392(1) Å	a = 8.3942(5) Å
	c = 5.204(1) Å	c = 5.1847(4) Å
V (Å^3)	317.39(8)	316.38(4)
Z	1	1
Absorption coefficient	48.784 mm^{-1}	47.938 mm^{-1}
F(000)	540	532
Crystal size	80 × 80 × 20 mm	70 × 35 × 20 mm
2θ range	5.60 to 60.08°	7.86 to 54.74°
Index ranges	$-11 \le h \le 11$	$-10 \le h \le 10$
	$-9 \le k \le 9$	$-10 \le k \le 10$
	$-7 \le l \le 7$	$-6 \le l \le 6$
Reflections collected/unique	1228/624	2467/483
	[R_{int} = 0.0225]	[R_{int} = 0.0605]
Refinement method	Full-matrix least-squares on F^2	Full-matrix least-squares on F^2
Goodness-of-fit on F^2	1.06	1.037
Final R indices [$F_o > 4\sigma F$]	0.0291, wR_2 = 0.0724	0.0330, wR_2 = 0.0617
R indices (all data)*	0.0328, wR_2 = 0.0745	0.0373, wR_2 = 0.0634
Extinction coefficient	0.002(7)	0.0000(7)
Largest diff. peak/hole (e/Å^3)	1.633/–1.358	1.341/–1.416
Flack parameter	0.025(15)	0.002(15)

Notes: $R_{int} = \Sigma|F_o^2 - F_o^2(\text{mean})|/\Sigma[F_o^2]$. GoF = $S = \{\Sigma[w(F_o^2 - F_c^2)^2]/(n-p)\}^{1/2}$. $R_1 = \Sigma||F_o| - |F_c||/\Sigma|F_o|$. $wR_2 = \{\Sigma[w(F_o^2 - F_c^2)^2]/\Sigma[w(F_o^2)^2]\}^{1/2}$. $w = 1/[\sigma^2(F_o^2) + (aP)^2 + bP]$ where a is 0.0434, b is 2.620 for Black Pine and a is 0, b is 0 for Blue Bell and where and P is $[2F_c^2 + \text{Max}(F_o^2, 0)]/3$.

displacement parameters are given in Table 4, polyhedral bond distances in Table 5, and a bond-valence analyses in Table 6.

Description of the structure

The crystal-structure determination shows that kuksite is isostructural with dugganite, $Pb_3Zn_3Te^{6+}As_2O_{14}$ (Lam et al. 1998) and joëlbruggerite, $Pb_3Zn_3(Sb^{5+},Te^{6+})As_2O_{13}(OH,O)$ (Mills et al. 2009). The dugganite crystal-structure type is comprised of heteropolyhedral ribbons of edge-sharing TeO_6 octahedra and PbO_8 disphenoids, oriented parallel to (0001). The sheets are cross-linked by PO_4 and ZnO_4 tetrahedra, which share corners to form an interlinked, two- and three-connected two-dimensional net parallel to (0001) (Fig. 2). The average bond lengths are typical for members of the group and correlate well with those of dugganite and joëlbruggerite. For the Black Pine crystal, <Pb-O> is 2.726 Å, <Zn-O> is 1.938 Å, <Te-O> is 1.924 Å, and <(P,As)-O> is 1.562 Å, while for the Blue Bell crystal, <Pb-O> is 2.724 Å, <Zn-O> is 1.947 Å, <Te-O> is 1.929 Å, and <(P,Si)-O> is 1.538 Å. The main difference between the two obtained structure models is that the Black Pine kuksite incorporates minor As into the tetrahedra, forming a partial solid solution toward dugganite, while the Blue Bell kuksite incorporates minor Si into the tetrahedra, in broad agreement with the chemical-analytical data (see above) and the unit-cell parameters refined from the powder data and single-crystal data (Tables 2 and 3, respectively). The chemistry suggests that some Sb might substitute for Te (as in joëlbruggerite); however, different crystals were used for chemical analyses. The result of the mentioned substitutions is that all oxygen atoms are fully occupied in the Black Pine structure (1.92 valence units, v.u., Table 4), whereas O3 is undersaturated in the Blue Bell structure (1.58 v.u., Table 6). The undersaturation of O3 matches that reported for joëlbruggerite (1.45 v.u., Mills et al. 2009). In the Black Pine structure, we attempted to refine the Te/Sb occupancy; however, the refinement was unstable and the BVS are ambiguous regarding the oxidation of the site, given that the bond-valence parameters for Te should be recalculated

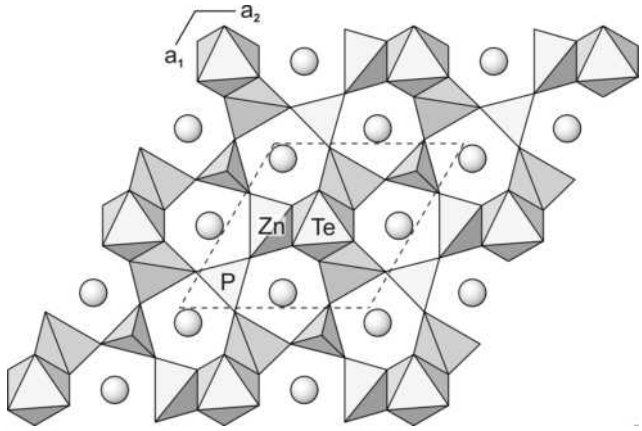

FIGURE 2. Crystal structure of kuksite projected onto (001). Pb atoms are indicated as spheres.

TABLE 4. Atomic coordinates and displacement parameters (Å²) for kuksite

	x/a	*y/b*	*z/c*	U_{eq}	U_{11}	U_{22}	U_{33}	U_{23}	U_{13}	U_{12}
					Black Pine					
Pb	0.40881(8)	0.0	0.0	0.0295(2)	0.0322(3)	0.0299(3)	0.0255(3)	0.0006(2)	0.00031(11)	0.01497(17)
Te	0.0	0.0	0.0	0.0224(5)	0.0254(6)	0.0254(6)	0.0164(8)	0.0	0.0	0.0127(3)
Zn	0.0	−0.2478(2)	0.5	0.0260(6)	0.0232(9)	0.0314(9)	0.0208(9)	0.0012(4)	0.0023(7)	0.0116(5)
(P,As)*	0.3333	−0.3333	0.5314(7)	0.0261(12)	0.0264(15)	0.0264(15)	0.026(2)	0.0	0.0	0.0132(7)
O1	−0.1224(13)	−0.2161(12)	0.7878(15)	0.036(2)	0.038(5)	0.040(5)	0.027(4)	−0.015(3)	0.005(3)	0.017(4)
O2	0.5251(15)	−0.1969(17)	0.6560(17)	0.056(3)	0.037(5)	0.067(7)	0.026(4)	−0.009(5)	0.009(4)	−0.001(5)
O3	0.3333	−0.3333	0.238(3)	0.038(3)	0.035(5)	0.035(5)	0.042(8)	0.0	0.0	0.018(3)
					Blue Bell					
Pb	0.4087(1)	0.0	0.0	0.0307(3)	0.0316(4)	0.0409(5)	0.0228(4)	0.0032(3)	0.0016(2)	0.0205(3)
Te	0.0	0.0	0.0	0.0194(5)	0.0248(7)	0.0248(7)	0.0086(9)	0.0	0.0	0.0124(4)
Zn	0.0	−0.2509(2)	0.5	0.0214(5)	0.0229(11)	0.0249(10)	0.0156(10)	−0.0005(5)	0.0011(9)	0.0114(6)
(P,Si)†	0.3333	−0.3333	0.5329(11)	0.022(3)	0.020(3)	0.020(3)	0.024(4)	0.0	0.0	0.010(2)
O1	−0.1229(13)	−0.2174(13)	0.7884(17)	0.034(3)	0.032(6)	0.041(7)	0.030(5)	−0.007(4)	−0.001(4)	0.018(5)
O2	0.5224(18)	−0.2023(17)	0.6613(24)	0.064(4)	0.046(7)	0.060(8)	0.051(8)	−0.006(6)	0.004(6)	0.001(7)
O3	0.3333	−0.3333	0.2456(34)	0.038(4)	0.039(7)	0.039(7)	0.035(10)	0.0	0.0	0.020(3)

* Refined occupancy: $P_{0.797(18)}As_{0.202(18)}$.
† Refined occupancy: $P_{0.67(58)}Si_{0.33(58)}$.

TABLE 5. Polyhedral bond distances (Å) in kuksite

		Black Pine	Blue Bell
Pb-O1	×2	2.393(9)	2.384(90)
Pb-O2	×2	2.768(15)	2.724(14)
Pb-O3	×2	2.827(7)	2.843(8)
Pb-O2	×2	2.915(13)	2.916(14)
<Pb-O>		2.726	2.717
Zn-O1	×2	1.908(8)	1.915(9)
Zn-O2	×2	1.968(10)	1.993(11)
<Zn-O>		1.938	1.954
Te-O1	×6	1.924(8)	1.928(9)
[P,(As/Si)]-O2	×3	1.574(10)	1.558(13)
[P,(As/Si)]-O3		1.525(16)	1.490(13)
<P(As/Si)-O>		1.562	1.564

TABLE 6. Bond-valence analyses (valence units) for kuksite

Black Pine	Pb	Te	Zn	(P,As)	Σ
O1	0.42 ↓×2	0.98 ↓×6	0.58 ↓×2		1.97
O2	0.19 ↓×2		0.49 ↓×2	1.23 ↓×3	2.06
	0.14 ↓×2				
O3	0.17 ↓×2			1.41	1.92
Σ	1.85	5.89	2.13	5.11	
Blue Bell	**Pb**	**Te**	**Zn**	**(P,Si)**	**Σ**
O1	0.48 ↓×2	0.97 ↓×6	0.57 ↓×2	2.02	
O2	0.19 ↓×2		0.46 ↓×2	1.17 ↓×3	2.00
	0.11 ↓×2				
O3	0.14 ↓×2			1.40	1.58
Σ	1.85	5.82	2.05	4.90	

Note: Calculated from Brown and Altermatt (1985) using refined occupancies and includes rounding errors.

with an independent *b* value (i.e., with $b \neq 0.37$). In the Blue Bell structure, the partially occupied H atom was not located; however, the evidence noted above suggests that it is most likely bonded to O3. The heterovalent substitution mechanism first proposed by Kim et al. (1988), where $As^{5+} \leftrightarrow Si^{4+}$ isomorphism is accomplished by $O^{2-} \leftrightarrow OH^{-}$ replacement, is consistent with the results obtained from the Blue Bell structure.

Discussion

Kim et al. (1990) described type kuksite as being orthorhombic, with possible space groups *Cmmm*, *C*222, *Cm*2*m*, or *Cmm*2, and noted that the *hk*0 and *hk*1 zones in their Weissenberg photographs did not correspond to the diffraction class 6/*mmm* [the original class assigned to dugganite by Williams (1978)]. Because it was later determined that dugganite has space-group symmetry *P*321 (Lam et al. 1998), we cannot unambiguously say whether Weissenberg photographs of Kim et al. (1990) can accommodate this symmetry. Kim et al. (1990) also determined type kuksite to be biaxial (–) with a 2*V* of 12–20°, which is consistent with orthorhombic symmetry. It is not clear whether stress alone could account for such a large deviation from uniaxial optics. It is possible that the crystals described by Kim et al. (1990) correspond to an orthorhombic polytype, "kuksite-*O*," whereas the Black Pine and Blue Bell kuksite correspond to a trigonal polytype, "kuksite-*T*." Symmetry reduction could occur as a result of substantial V/Si substitution for P/As {type kuksite contains substantial V and Si, the empirical formula being $(Pb_{2.68}Ca_{0.31})_{\Sigma 2.99}Zn_{3.01}Te_{0.96}O_{5.94}[(P_{0.86}V_{0.12}Si_{0.04})_{\Sigma 1.02}O_4]_2$; Kim et al. (1990)}. Extensive examinations of material from the type specimen, obtained from Yakutsk Institute (catalog no. Mk-112), failed to confirm the presence of any kuksite, so we are unable to experimentally confirm this hypothesis. We note, however, that several synthetic dugganite-like compounds exist (Mill' 2009a, 2009b), all with *P*321 symmetry and that orthorhombic symmetry, has yet to be confirmed by single-crystal studies of natural or synthetic samples. Cheremnykhite, the V analog of kuksite, was also described as orthorhombic by Kim et al. (1990); however, it too may possibly be trigonal. We were unable to acquire a sample of cheremnykhite for further studies.

A note on the crystal structure of yafsoanite

While we were unable to find any kuksite in the material from the type specimen noted above, we did encounter somewhat rounded, brown, glassy, transparent grains of yafsoanite, $(Ca,Pb)_3Te_2^{6+}Zn_3O_{12}$, which was first described by Kim et al. (1982) also from the Delbe orebody. Rozhdestvenskaya et al. (1984) first determined the structure of yafsoanite in space group $I4_132$, while Jarosch and Zemann (1989) showed the mineral to have the garnet structure, with space group $Ia\bar{3}d$. Because the latter authors noted their crystal as "very far from being ideal," we decided to collect a new set of structure data and try to obtain an improved structure refinement. An irregular $86 \times 73 \times 53$ μm crystal was used for the data collection on a Rigaku R-Axis Spider curved imaging plate microdiffractometer utilizing monochromatized Mo*K*α radiation. The Rigaku CrystalClear software package was used for processing of the structure data. An empirical absorption correction was applied. The SHELXL-97 software (Sheldrick 2008) was used for the refinement of the structure. The details of the data collection and the final structure refinement are provided in Table 7, the final atomic coordinates and displacement parameters in Table 8, and selected interatomic distances in Table 9.

Our refinement confirms the model described by Jarosch and Zemann (1989) with a significant improvement in the quality of R_1 (2.41 vs. 7.5%) and the precision of the atomic positions and bond lengths. We did not encounter the anomaly in the weighted *R* noted by Jarosch and Zemann (1989) for their refinement for which *wR* (2.8%) was much lower than R_1.

The empirical formula reported by Kim et al. (1982) in the original description of yafsoanite was $(Zn_{1.38}Ca_{1.36}Pb_{0.26})_3TeO_6$. As noted by Rozhdestvenskaya et al. (1984) and by Jarosch and Zemann (1989), the small amount of Pb must occupy the eightfold-coordinated Ca site. Our refined occupancy for the site is $Ca_{0.912}Pb_{0.088}$, indicating somewhat lower Pb content than either the refinement by Jarosch and Zemann, $Ca_{0.86}Pb_{0.14}$, or that suggested by the empirical formula, $Ca_{0.83}Pb_{0.17}$. Fitting the empirical formula to the structure is rather problematic because, after assigning all Pb to the Ca site, there remains an excess of Ca, which does not appear compatible with either the octahedral Te site (<Te-O> = 1.928 Å) or the tetrahedral Zn site (<Zn-O> =

Table 7. Summary of data collection conditions and refinement parameters for yafsoanite

Structural formula	$(Ca_{2.74}Pb_{0.26})_{\Sigma 3}Te_2^{6+}Zn_{2.87}O_{12}$
Temperature	298(2) K
X-ray radiation/power	MoKα (λ = 0.710747 Å)/50 kV, 40 mA
Space group	$Ia\bar{3}d$
a	12.6350(7) Å
Z	8
V	2017.1(2) Å^3
Density (for formula above)	5.441 g/cm^3
Absorption coefficient	20.381 mm^{-1}
F(000)	2986
Crystal size	$86 \times 73 \times 53$ μm
2θ range	7.90 to 54.60°
Index ranges	$-15 \le h \le 16$, $-15 \le k \le 12$, $-10 \le l \le 16$
Reflections collected/unique	2598/193 [$R_{int} = 0.035$]
Reflections with $F_o > 4\sigma F$	135
Refinement method	Full-matrix least-squares on F^2
Parameters refined	19
Goodness-of-fit on F^2	1.033
Final *R* indices [$F_o > 4\sigma F$]	$R_1 = 0.0241$, $wR_2 = 0.0617$
R indices (all data)	$R_1 = 0.0368$, $wR_2 = 0.0680$
Largest diff. peak/hole	+0.63/–0.42 *e*/A^3

Notes: $R_{int} = \Sigma|F_o^2 - F_o^2(\text{mean})|/\Sigma[F_o^2]$. GoF = $S = \{\Sigma[w(F_o^2 - F_c^2)^2]/(n-p)\}^{1/2}$. $R_1 = \Sigma||F_o| - |F_c||/\Sigma|F_o|$. $wR_2 = \{\Sigma[w(F_o^2 - F_c^2)^2]/\Sigma[w(F_o^2)^2]\}^{1/2}$. $w = 1/[\sigma^2(F_o^2) + (aP)^2 + bP]$ where *a* is 0.0371, *b* is 0, and *P* is $[2F_c^2 + \text{Max}(F_o^2,0)]/3$.

Table 8. Atomic coordinates and displacement parameters (Å^2) for yafsoanite

	x/a	*y/b*	*z/c*	U_{eq}	U_{11}	U_{22}	U_{33}	U_{23}	U_{13}	U_{12}
(Ca,Pb)*	0.0	0.25	0.125	0.0179(7)	0.0160(8)	0.0160(8)	0.0217(10)	0.0	0.0	0.0034(5)
Te	0.0	0.0	0.0	0.0097(3)	0.0097(3)	0.0097(3)	0.0097(3)	0.0007(2)	0.0007(2)	0.0007(2)
Zn*	0.0	0.25	0.375	0.0131(5)	0.0141(5)	0.0141(5)	0.0111(7)	0.0	0.0	0.0
O	–0.0273(2)	0.0489(3)	0.1419(2)	0.0149(7)	0.012(2)	0.017(2)	0.016(2)	–0.001(1)	0.003(1)	0.000(1)

* (Ca,Pb) occupancy: Ca = 0.912(3), Pb = 0.088(3); Zn occupancy = 0.957(6).

TABLE 9. Selected bond lengths (Å) for yafsoanite

(Ca,Pb)-O	×4	2.439(3)
(Ca,Pb)-O	×4	2.573(3)
<(Ca,Pb)-O>		2.506
Te-O	×6	1.927(3)
Zn-O	×4	1.943(3)

1.941 Å). In our refinement, the Te site refines to full occupancy and the Zn site to slightly less than full occupancy (0.957). While the latter could imply a small amount of Ca at the Zn site, this would require unreasonably short Ca-O distances. We suggest that the most likely explanation is that the original chemical analysis by Kim et al. (1982) is in error.

ACKNOWLEDGMENTS

The Associate Editor, Darrell Henry, Peter Williams, and an anonymous reviewer provided helpful comments on the manuscript that are greatly appreciated. Mihail Tomshin (Yaktusk Institute) is thanked for providing a sample for study and Andrey Bulakh for help receiving the sample. NSERC Canada is thanked for a Discovery Grant to Mati Raudsepp. Part of this study was funded by the John Jago Trelawney Endowment to the Mineral Sciences Department of the Natural History Museum of Los Angeles County. Jean-Marc Johannet is thanked for providing a photograph of kuksite.

REFERENCES CITED

Brown, I.D. and Altermatt, D. (1985) Bond-valence parameters obtained from a systematic analysis of the inorganic crystal structure database. Acta Crystallographica, B41, 244–247.

Burns, P. (2000) Quetzalcoatlite; A new octahedral-tetrahedral structure from a 2 × 2 × 40 cubic micrometer crystal at the Advanced Photon Source-GSE-CARS Facility. American Mineralogist, 85, 604–607.

Crowley, J.A. (1977) Minerals of the Blue Bell mine, San Bernardino County, California. Mineralogical Record, 8, 494–496.

Fadda, S., Fiori, M., and Grillo, S.M. (2005) Chemical variations in tetrahedrite-tennantite minerals from the Furtei epithermal au deposit, Sardinia, Italy: Mineral zoning and ore fluids evolution. Au-Ag-Te-Se deposits, IGCP Project 486, 2005 Field Workshop, Kiten, Bulgaria, 79–84.

Grundler, P., Brugger, J., Meisser, N., Ansermet, S., Borg, S., Etschmann, B., Testemale, D., and Bolin, T. (2008) Xocolatlite, $Ca_2Mn^{4+}_2Te_2O_{12}\cdot H_2O$, a new tellurate related to kuranakhite: Description and measurement of Te oxidation state by XANES spectroscopy. American Mineralogist, 93, 1911–1920.

Housley, R.M. (1997) Recent discoveries of tlalocite, kuksite, and other rare minerals from the Blue Bell mine, San Bernardino County, California. San Bernardino County Museum Association Quarterly, 44, 9–12.

Jarosch, D. and Zemann, J. (1989) Yafsoanite: A garnet type calcium-tellurium(VI)-zinc oxide. Mineralogy and Petrology, 40, 111–116.

Kampf, A.R., Housley, R.M., Mills, S.J., Marty, J., and Thorne, B. (2010) Lead-tellurium oxysalts from Otto Mountain near Baker, California: I. Ottoite, Pb_2TeO_5, a new mineral with chains of tellurate octahedra. American Mineralogist, 95, in press.

Kim, A.A., Zayakina, N.V., and Lavrent'ev, Y.G. (1982) Yafsoanite—$(Zn_{1.38}Ca_{1.36}Pb_{0.26})_3TeO_6$, a new tellurium mineral. Zapiski Vsesoyuznogo Mineralogicheskogo Obshchestva, 111, 118–121 (in Russian).

Kim, A.A., Zayakina, N.V., Lavrent'ev, Yu.G., and Makhotko, V.F. (1988) Vanadian silician variety of dugganite: First find in the USSR. Mineralogicheskii Zhurnal, 10, 85–89 (in Russian).

Kim, A.A., Zayakina, N.V., and Mahkotko, V.F. (1990) Kuksite $Pb_3Zn_3Te^{6+}O_6(PO_4)_2$ and cheremnykhite $Pb_3Zn_3Te^{6+}O_6(VO_4)_2$—New tellurates from the Kuranakh gold deposit (Central Aldan, southern Yakutia). Zapiski Vsesoyuznogo Mineralogicheskogo Obshchestva, 119, 50–57 (in Russian).

Lam, A.E., Groat, L.A., and Ercit, T.S. (1998) The crystal structure of dugganite, $Pb_3Zn_3TeAs_2O_{14}$. Canadian Mineralogist, 36, 823–830.

Laugier, J. and Bochu, B. (2004) Chekcell: Graphical powder indexing cell and space group assignment software. http://www.ccp14.ac.uk/tutorial/lmgp/.

Maynard, M.F. (1984) The Blue Bell Claims, San Bernardino County, California. San Bernardino County Museum, Department of Earth Sciences, Redlands, California.

Mill', B.V. (2009a) Synthesis of dugganite $Pb_3TeZn_3As_2O_{14}$ and its analogues. Russian Journal of Inorganic Chemistry, 54, 1205–1209.

——— (2009b) New compounds (A = Na, K; M = Ga, Al, Fe; X = P, As, V) with the $Ca_3Ga_2Ge_4O_{14}$ structure. Russian Journal of Inorganic Chemistry, 54, 1355–1357.

Mills, S.J., Kolitsch, U., Miyawaki, R., Groat, L.A., and Poirier, G. (2009) Joëlbruggerite, $Pb_3Zn_3(Sb^{5+},Te^{6+})As_2O_{13}(OH,O)$, the Sb^{5+} analogue of dugganite, from the Black Pine mine, Montana. American Mineralogist, 94, 1012–1017.

Mills, S.J., Kampf, A.R., Poirier, G., Raudsepp, M., and Steele, I.M. (2010) Auricusite, $Fe^{3+}Cu^{2+}AsO_4O$, the first M^{3+} member of the olivenite group, from the Black Pine mine, Montana, U.S.A. Mineralogy and Petrology, 99, 113–120, DOI: 10.1007/s00710-009-0089-7.

Otwinowski, Z. and Minor, W. (1997) Processing of X-ray diffraction data collected in oscillation mode. In C.W. Carter, Jr. and R.M. Sweet, Eds., Methods in Enzymology, 276, p. 307–326. Macromolecular Crystallography A, Academic Press, New York.

Otwinowski, Z., Borek, D., Majewski, W., and Minor, W. (2003) Multiparametric scaling of diffraction intensities. Acta Crystallographica, A59, 228–234.

Peacor, D.R., Dunn, P.J., Ramik, R.A., Sturman, B.D., and Zeihan, L.G. (1985) Philipsburgite, a new copper zinc arsenate hydrate related to kipushite, from Montana. Canadian Mineralogist, 23, 255–258.

Rozhdestvenskaya, I.V., Zajakina, N.V., and Kim, A.A. (1984) The crystal structure of the Zn-Ca-Tellurate yafsoanite. Mineral Shurnal, 6, 75–79 (in Russian).

Sheldrick, G.M. (2008) A short history of *SHELX*. Acta Crystallographica, A64, 112–122.

Williams, S.A. (1978) Khinite, parakhinite, and dugganite, three new tellurates from Tombstone, Arizona. American Mineralogist, 63, 1016–1019.

MANUSCRIPT RECEIVED DECEMBER 23, 2009
MANUSCRIPT ACCEPTED MARCH 17, 2010
MANUSCRIPT HANDLED BY DARRELL HENRY